Frontoparietal network integrity supports cognitive function despite atrophy and hypoperfusion in pre-symptomatic frontotemporal dementia: multimodal analysis of brain function, structure and perfusion

Xulin Liu[1], P Simon Jones[1], Maurice Pasternak,[2,3] Mario Masellis,[2,3] Arabella Bouzigues,[4] Lucy L. Russell,[4] Phoebe H. Foster,[4] Eve Ferry-Bolder,[4] John van Swieten,[5] Lize Jiskoot,[5] Harro Seelaar,[5] Raquel Sanchez-Valle,[6] Robert Laforce,[7] Caroline Graff,[8,9] Daniela Galimberti,[10,11] Rik Vandenberghe,[12,13] Alexandre de Mendonça,[14] Pietro Tiraboschi,[15] Isabel Santana,[16,17] Alexander Gerhard,[18,19,20] Johannes Levin,[21,22,23] Sandro Sorbi,[24,25] Markus Otto,[26] Florence Pasquier,[27,28,29] Simon Ducharme,[30,31] Chris Butler,[32,33] Isabelle Le Ber,[34,35,36] Elizabeth Finger,[37] Maria Carmela Tartaglia,[38] Matthis Synofzik,[39,40] Fermin Moreno,[41, 42] Barbara Borroni,[43] Jonathan D. Rohrer,[4] Kamen A. Tsvetanov*,[1,44] James B. Rowe*,[1,45] and The GENFI consortium[#].

1 Department of Clinical Neurosciences and Cambridge University Hospitals NHS Trust, University of Cambridge, Cambridge, UK
2 Sunnybrook Health Sciences Centre, Sunnybrook Research Institute, Toronto, Canada
3 University of Toronto, Toronto, Canada
4 Dementia Research Centre, Department of Neurodegenerative Disease, UCL Institute of Neurology, Queen Square, London, UK
5 Department of Neurology, Erasmus Medical Centre, Rotterdam, The Netherlands
6 Alzheimer's disease and Other Cognitive Disorders Unit, Neurology Service, Hospital Clínic, Institut d'Investigacións Biomèdiques August Pi I Sunyer, University of Barcelona, Barcelona, Spain
7 Clinique Interdisciplinaire de Mémoire, Département des Sciences Neurologiques, CHU de Québec, and Faculté de Médecine, Université Laval, Québec, Canada
8 Karolinska Institute, Department NVS, Centre for Alzheimer Research, Division of Neurogenetics, Stockholm, Sweden
9 Unit for Hereditary Dementias, Theme Aging, Karolinska University Hospital, Solna, Sweden
10 Fondazione IRCSS Ca' Granda, Ospedale Maggiore Policlinico, Neurodegenerative Diseases Unit, Milan, Italy
11 University of Milan, Centro Dino Ferrari, Milan, Italy
12 Laboratory for Cognitive Neurology, Department of Neurosciences, KU Leuven, Leuven, Belgium
13 Neurology Service, University Hospitals Leuven, Belgium
14 Faculty of Medicine, University of Lisbon, Lisbon, Portugal
15 Fondazione IRCCS Istituto Neurologico Carlo Besta, Milano, Italy
16 Faculty of Medicine, University of Coimbra, Coimbra, Portugal
17 Centre of Neurosciences and Cell biology, University of Coimbra, Coimbra, Portugal
18 Division of Psychology Communication and Human Neuroscience, Wolfson Molecular Imaging Centre, University of Manchester, Manchester, UK
19 Department of Nuclear Medicine, Centre for Translational Neuro- and Behavioral Sciences, University Medicine Essen, Essen, Germany
20 Department of Geriatric Medicine, Klinikum Hochsauerland, Arnsberg, Germany
21 Department of Neurology, Ludwig-Maximilians Universität München, Munich, Germany
22 Centre for Neurodegenerative Diseases (DZNE), Munich, Germany
23 Munich Cluster of Systems Neurology, Munich, Germany
24 Department of Neurofarba, University of Florence, Italy
25 IRCCS Fondazione Don Carlo Gnocchi, Florence, Italy
26 Department of Neurology, University of Ulm, Germany
27 University Lille, Lille, France
28 Inserm 1172, Lille, France
29 CHU, CNR-MAJ, Labex Distalz, LiCEND Lille, France
30 Department of Psychiatry, McGill University Health Centre, McGill University, Montreal, Canada
31 McConnell Brain Imaging Centre, Montreal Neurological Institute, McGill University, Montreal, Canada
32 Nuffield Department of Clinical Neurosciences, Medical Sciences Division, University of Oxford, Oxford, UK
33 Department of Brain Sciences, Imperial College London, UK
34 Sorbonne Université, Paris Brain Institute – Institut du Cerveau – ICM, Inserm U1127, CNRS UMR 7225, AP-HP - Hôpital Pitié-Salpêtrière, Paris, France
35 Centre de référence des démences rares ou précoces, IM2A, Département de Neurologie, AP-HP - Hôpital Pitié-Salpêtrière, Paris, France
36 Département de Neurologie, AP-HP - Hôpital Pitié-Salpêtrière, Paris, France
37 Department of Clinical Neurological Sciences, University of Western Ontario, London, ON, Canada
38 Toronto Western Hospital, Tanz Centre for Research in Neurodegenerative Disease, Toronto, Ontario, Canada
39 Department of Neurodegenerative Diseases, Hertie-Institute for Clinical Brain Research & Centre of Neurology, University of Tübingen, Germany
40 Centre for Neurodegenerative Diseases (DZNE), Tübingen, Germany
41 Cognitive Disorders Unit, Department of Neurology, Hospital Universitario Donostia, San Sebastian, Gipuzkoa, Spain
42 Neuroscience Area, Biodonostia Health Research Institute, San Sebastian, Gipuzkoa, Spain
43 Neurology Unit, Department of Clinical and Experimental Sciences, University of Brescia, Brescia, Italy
44 Department of Psychology, University of Cambridge, Cambridge, UK
45 MRC Cognition and Brain Science Unit, University of Cambridge, Cambridge, UK
**joint senior authors*

Correspondence: Xulin Liu xl454@cam.ac.uk
University of Cambridge Department of Clinical Neurosciences,
Herchel Smith Building, Cambridge Biomedical Campus, CB2 0SZ United Kingdom

ABSTRACT

INTRODUCTION: Gene carriers of frontotemporal dementia can remain cognitively well despite neurodegeneration. A better understanding of brain structural, perfusion and functional patterns in pre-symptomatic stage could inform accurate staging and potential mechanisms.

METHODS: We included 207 pre-symptomatic carriers and 188 relatives without mutations. The grey matter volume, cerebral perfusion, and resting-state functional network maps were co-analyzed using linked independent component analysis (LICA). Multiple regression analysis was used to investigate the relationship of LICA components to genetic status and cognition.

RESULTS: Pre-symptomatic carriers showed an age-related decrease in the left frontoparietal network integrity while non-carriers did not. Executive functions of pre-symptomatic carriers became dependent on the left frontoparietal network integrity in older age.

DISCUSSION: The frontoparietal network integrity of pre-symptomatic carriers showed a distinctive relationship to age and cognition compared to non-carriers, despite atrophy and hypoperfusion. Functional network integrity may contribute to brain resilience, mitigating the effects of atrophy and hypoperfusion.

1. Background

Frontotemporal dementia (FTD) is characterized by the selective degeneration of the frontal and temporal cortices, leading to progressive deficits in behavior, social and executive function, or language [1]. Genetic risk factors are important, with about 20-30% of FTD cases being familial [2]. Highly penetrant mutations in three major genes, chromosome 9 open reading frame 72 (*C9orf72*), microtubule-associated protein tau (*MAPT*), and progranulin (*GRN*), account for about 60% of cases of familial FTD [1]. Given that neurobiological changes could occur many years before the onset of symptoms of neurodegenerative dementias [3-6], investigation at the early stage of diseases before symptom onset is important for understanding factors that facilitate the brain's resilience. Genetic FTD with highly penetrant genetic mutations provides the opportunity for early investigation before symptom onset. Comparison between pre-symptomatic genetic mutation carriers and their family members without the mutation, allows one to investigate the effect of early neurodegeneration without the confounding influence of medication and lifestyle changes after symptom onset.

People carrying highly penetrant genetic mutations of FTD have grey matter atrophy and reduction in cerebral blood flow (CBF) more than a decade before the expected symptom onset, as measured by magnetic resonance imaging (MRI) and arterial spin labelling (ASL)[4, 6-8]. However, functional network organization and connectivity are generally maintained despite significant atrophy in pre-symptomatic genetic FTD [4, 9]. Moreover, a recent study indicates that functional networks predict cognitive decline and symptomatic conversion in pre-symptomatic genetic mutation carriers [10]. A better understanding of these changes in the pre-symptomatic stage would inform accurate staging, facilitate clinical trials, and elucidate the

mechanisms of resilience by which gene carriers remain cognitively well for many years despite biomarker evidence of neurodegeneration.

Here we test whether pre-symptomatic differences in brain structure, cerebral perfusion and functional network act synergistically or independently on clinically relevant disease features such as cognitive performance and disease progression. Specifically, we used linked independent components analysis of multimodal imaging to investigate whether the interplay of brain grey matter atrophy, cerebral perfusion and functional network integrity explains difference between pre-symptomatic FTD genetic mutation carriers and non-carriers.

2. Methods

2.1 Participants

The Genetic Frontotemporal dementia Initiative (GENFI) study is an international muti-centre cohort study across Europe and Canada. GENFI recruited participants with genetic mutations of FTD and their relatives [6, 7]. Participants included carriers of genetic mutations in *C9orf72*, *GRN*, and *MAPT* who have or have not shown symptoms, and their relatives without genetic mutations. Most participants are unaware of their genetic status at recruitment, and remain unaware of their genetic status by a genetic-guardianship process. Participants underwent a standardized clinical assessment consisting of a medical history, family history, and physical examination. Symptomatic status was based on the assessment by clinicians to determine whether the participants fulfilled the diagnosis criteria for FTD [11-13]. Functional status was measured using the Frontotemporal Dementia Rating Scale [14] and behavioral symptoms were assessed using the Cambridge Behavioural Inventory Revised version (CBI-R) [15]. We also tested the Mini-Mental State Examination (MMSE). Participants who had functional,

cerebrovascular and structural neuroimaging data with good quality were included in this study (N = 395) – 207 genetic mutation carriers who had not shown symptoms fulfilling the diagnosis criteria for FTD at the time of recruitment, termed pre-symptomatic carriers; and 188 relatives of the carriers who are not genetic mutation carriers of known FTD genes, termed non-carriers. The demographics of the subjects are shown in **Table 1**. Demographic variables were compared between pre-symptomatic carriers and non-carriers using one-way Analysis of Variance (ANOVA) for continuous variables and using the Chi-squared test for categorical variables.

Table 1. Characteristics of participants.

	Non-carriers	**Pre-symptomatic carriers**	***P* value (Chi-squared or ANOVA)**
n	188	207	
Age, mean±SD	45.6±12.1	44.1±11.6	0.23
Gender, n(%)			
Females	117 (62.2)	139 (67.1)	0.29
Males	71 (37.8)	68 (32.9)	
Gene, n(%)			
C9orf72	62 (33.0)	76 (36.7)	
GRN	83 (44.1)	97 (46.9)	0.14
MAPT	43 (22.9)	34 (16.4)	
Mini-Mental State Examination, mean±SD	29.4±1.0	29.4±1.0	0.49
Cambridge Behavioural Inventory, mean±SD	4.6±7.0	6.1±9.7	0.10

2.2 Neurocognitive assessment

Participants underwent a neuropsychological battery consisting of tests from the Uniform Data Set [16], covering attention and processing speed: Wechsler Memory Scale–Revised (WMS-R) digit span forward [16], Trail-Making Test part A (TMTA) [17], the Wechsler Adult Intelligence Scale-Revised (WAIS-R) Digit Symbol Substitution test [16], Delis-Kaplan Executive Function System (DKEFS) Color-Word Interference Test color and word naming [18]; executive function: WMS-R Digit span backward [16], TMT part B (TMTB) [17], DKEFS Color-Word Interference Test ink naming [18]; language: modified Camel and Cactus Test [19], the Boston Naming Test (short 30-item version) [16], verbal fluency: category fluency and phonemic fluency [16, 20]; memory encoding: Free and Cued Selective Reminding Test (FCSRT) immediate free and total recall [21]; memory recall: FCSRT delayed free and total recall, Benson Complex Figure recall [21]; and visuoconstruction: Benson Complex Figure copy. More details of the neurocognitive assessment in this cohort can also be found in the previously published protocol [6]. A principal component analysis (PCA) with permutation (n = 1000) was performed on the series of cognitive measures. Leading components were selected for further investigation.

2.3 Neuroimaging acquisition and processing

2.3.1 Grey matter volume

T1-weighted MRI scans were collected on 3T scanners. A three-dimensional T1-weighted magnetization prepared rapid gradient echo sequence image was acquired for each subject accommodating different scanners at each site over at least 283 s (283 to 462 s) and had a median isotropic resolution of 1.1 mm (1 to 1.3 mm), repetition time (TR) of 2000 ms (6.6 to 2400), echo time (TE) of 2.9 ms (2.6 to 3.5 ms), inversion time of 8 ms (8 to 9 ms), and field of

view (FOV) 256 × 256 × 208 mm (192 to 256 × 192 to 256 × 192 to 208 mm). For participants with baseline and follow-up scans, the latest available scans were examined. The co-registered T1 images were segmented to extract probabilistic maps of six tissue classes: grey matter, white matter, cerebrospinal fluid, bone, soft tissue, and residual noise. The native-space grey matter and white matter images were submitted to diffeomorphic registration to create equally represented gene-group template images [22]. The templates for all tissue types were normalized to the Montreal Neurological Institute (MNI) template using a 12-parameter affine transformation. The normalized and modulated grey matter volume (GMV) images were used in analysis.

2.3.2 CBF

ASL sequences could be different across different sites. The sequences included in this study were: pseudo-continuous ASL 3D fast-spin-echo stack-of-spirals implemented on a 3T General Electric MR750; pseudo-continuous ASL 2D gradient-echo echo-planar imaging on a 3T Philips Achieva, with and without background suppression; and pulsed ASL 3D gradient-and-spin-echo on 3T Siemens Trio systems. The complete ASL parameters of each sequence have been described elsewhere [23].

For ASL processing, the ExploreASL pipeline (v1.5.1) was used [24]. Structural and functional image volumes across multiple sites, vendors, and sequences were processed first. Briefly, structural images were non-linearly registered to MNI space using Geodesic Shooting [25] and transformation matrices were saved for subsequent application on functional images. ASL scans were corrected for motion outliers using rigid-body transformation coupled with the enhancement of automated blood flow estimates outlier exclusion algorithm [26], followed by

pairwise subtraction to produce perfusion-weighted images. Functional proton-density weighted images were smoothed with a 16mm full width at half maximum (FWHM) Gaussian kernel to create a bias field that avoided division artifacts during CBF quantification and cancelled out acquisition-specific B1-field inhomogeneities. CBF quantification itself followed a single-compartment model approach and recommendations outlined in the ASL consensus paper [27]. For quality control, CBF images were reviewed independently by three authors with 3-6 years of experience in handling ASL data. Disagreements were resolved by consensus. CBF volumes were masked by their structural T1 counterpart's probability grey matter mask at ≥ 50% and the spatial coefficient of variation was calculated for the extracted voxels. Images with coefficient of variation values ≥ 0.8 were discarded.

To adjust for differences arising from the effects of multiple sites, scanners, and software, a spatially varying intensity normalization approach was used [8]. This approach uses the within-site CBF similarity between participants to remove the between-site quantification differences [8]. Mean CBF images of these groupings were calculated and smoothed using a 6.4mm FWHM Gaussian kernel. Smoothing was constrained to a binary MNI brain mask. These group-specific mean images were then averaged to calculate the population mean CBF image, which in turn was rescaled uniformly such that the mean grey matter perfusion equalled 60 ml / min / 100 g. Group-specific rescale-factor images were then calculated by dividing this population CBF image by each group's mean CBF image. Individual CBF images were adjusted via multiplication against their group's respective rescale-factor image. To account for the effects of atrophy, partial volume correction on rescaled CBF volumes was performed using a linear regression approach [28]. Further details of ASL processing are discussed in a recent publication [29]. Due to hyperintensities present in the cerebellum of many subjects which is not our interest

of study, only the CBF of the cortical region was included in the analysis of this study. A cortical binary mask created from the Harvard-Oxford cortical atlas (https://fsl.fmrib.ox.ac.uk/fsl/fslwiki/Atlases) was therefore applied to all CBF images.

2.3.3 Resting-state functional networks

For rs-fMRI, echo planar imaging acquired 200 volumes with 42 slices (slice thickness = 3.5 mm, TR = 2500 ms; TE = 30 ms; FOV = 192 mm x 192 mm). Resting-state fMRI data were preprocessed using Automatic Analysis [30] calling functions from SPM12 implemented in Matlab (MathWorks). Processing steps included (1) spatial realignment to correct for head movement and movement by distortion interactions, (2) temporal realignment of all slices, and (3) coregistration of the echo planar imaging to the participant's T1 anatomical scan. The normalization parameters from the T1 stream were applied to warp functional images into MNI space. Resting-state fMRI data were further processed using whole-brain ICA of single-subject time series denoising, with noise components selected and removed automatically using the ICA-based Automatic Removal of Motion Artifacts toolbox [31, 32]. This was complemented with linear detrending of the fMRI signal, covarying out six realignment parameters, white matter and cerebrospinal fluid signals, their first derivatives, and quadratic terms [33]. Global white matter and cerebrospinal fluid signals were estimated for each volume from the mean value of white matter and cerebrospinal fluid masks derived by thresholding SPM tissue probability maps at 0.75. Data were band-pass filtered using a discrete cosine transform.

In order to identify the activation of functional networks from rs-fMRI, group-level ICA was performed to decompose the rs-fMRI data (trendscenter.org/software/gift/) [34] from 395 participants (including pre-symptomatic mutation carriers and non-carriers). ICA dissociates

signals from complex datasets with minimal assumptions [35], to represent data in a small number of independent components (ICs) which here are spatial maps that describe the temporal and spatial characteristics of underlying signals [34, 36]. The values at each voxel reflect the correlation between the time series of the voxel and that of the component. Each component can therefore be interpreted as BOLD co-activation across voxels of a functional network at resting state [37]. The number of components used, N = 15, matched a common degree of decomposition previously applied in low-dimensional group-ICA of rs-fMRI [38-40] and generated network spatial maps that showed a high degree of overlapping with network templates. Low-dimensional group-ICA was used because the purpose was to define each network with a single component, and high-dimensional group-ICA would tend to decompose single network into multiple components. The stability of the estimated ICs was evaluated across 100 ICASSO iterations [41]. Functional networks were identified from components by visualization and validated by spatially matching the components to pre-existing templates [42], in accordance with the previous methodology used to identify networks from ICs [43, 44]. The dorsal and ventral default mode network, the salience network, and the left and right frontoparietal network were selected, which are higher-order functional networks known to be associated with age- and FTD-related cognitive change [45-47].

2.4 Statistical analysis

2.4.1 Linked ICA

Linked independent component analysis (ICA) was performed using FLICA of FMRIB (https://fsl.fmrib.ox.ac.uk/fsl/fslwiki/FLICA) [48, 49] implemented in Matlab (MathWorks version 2021b). Linked ICA is a data-driven analytic method that allows for simultaneous

characterization of multimodal imaging modalities while taking into account the covariance across imaging modalities [48]. In comparison with other commonly used multivariate approaches such as canonical correlation analysis and partial least squares, linked ICA is able to identify patterns of covariance across more than two modalities. Linked ICA was run with seven spatial map inputs: GMV, CBF, and five co-activation maps from resting-state functional networks (i.e., the dorsal default mode network, the ventral default mode network, the salience network, the right frontoparietal network and the left frontoparietal network) identified as described in 2.3.3. To ensure the results were not influenced dominantly by non-grey matter regions (e.g., ventricles), all spatial maps were masked by thresholding SPM grey matter tissue probability maps at 0.3. We refer to these imaging-derived spatial maps as modalities in linked ICA. A summary flow chart of the processing and analysis of imaging modalities is presented in **Figure 1**.

Within each modality, images from all subjects were concatenated into a single input matrix (participants-by-voxels) for linked ICA. Linked ICA decomposed this n-by-m matrix of participants-by-voxels into spatial components, with each component being an aggregate of spatial patterns, one for each modality, along with a set of subject loadings, one for each component (for more details see [48, 50]). Each modality spatial pattern is a map of weights that is later converted to pseudo-Z-statistic by accounting for the scaling of the variables and the signal-to-noise ratio in that modality. Only modalities with significant contribution (i.e., weighting with Z-score > 3.34, which corresponds to $P < 0.001$) were presented in this study. Linked ICA subject loadings for a given component were shared among all modalities represented in that component and indicated the degree to which that component was expressed

by any individual subject. Subject loadings were used as inputs to the second-level between-subject regression analysis (see below in 2.4.2).

2.4.2 Multiple regression analysis

To investigate the effects of age (linear and quadratic) and genetic mutation on cognition, multiple regression analysis was used with cognition PCA component scores as the dependent variable. Group was classified by genetic mutation status (i.e., pre-symptomatic carriers or non-carriers). Gender and site effect were included as covariates. In Wilkinson's notation [51], the model took the form:

*Cognition component ~ Group*Age^2 + Gender + site*.

To investigate whether brain patterns were predicted by age (linear and quadratic), genetic mutation and their interaction, subject loadings of each linked ICA component (IC) of interest were investigated as the dependent variable in multiple regression. Gender, total brain volume and site effect were included as covariates. In Wilkinson's notation, the model took the form:

*IC ~ Group*Age^2 + Gender + total brain volume + site*.

Finally, to investigate the relationship between brain patterns and cognitive variability, accounting for the effects of genetics and age (linear and quadratic), multiple regression was used taking the following form:

*Cognition component ~ IC*Group*Age^2 + Gender + total brain volume + site*.

A false discovery rate (FDR)-corrected $P < 0.05$ was considered statistically significant. Analyses were performed in Matlab.

3. Results

3.1 Relationship between age, gene group and cognitive function

The two significant PCA components are shown in **Figure 2**. The first cognition component (variance explained 36.6%, $P < 0.001$) was related to global cognitive function. No significant group-wise difference in global cognition was found between genetic mutation carriers and non-carriers ($P = 0.079$). Both non-carriers and pre-symptomatic genetic mutation carriers showed a decline in global cognition with age likely reflecting the general age-related decrease in global cognitive function. No significant difference was found in the age-cognition relationship between genetic mutation carriers and non-carriers (Group:Age interaction t = -0.97, $P = 0.33$; Group:Age^2 interaction t = -0.73, $P = 0.47$).

The second cognition component (variance explained 9.1%, $P < 0.001$) indicated executive function, attention and processing speed with deficits in visuospatial memory. No significant group-wise difference was found between genetic mutation carriers and non-carriers ($P = 0.28$). Neither non-carriers nor pre-symptomatic genetic mutation carriers showed age-related changes in these cognitive functions. No significant difference was found in the age-cognition relationship between genetic mutation carriers and non-carriers (Group:Age interaction t = -0.62, $P = 0.53$; Group:Age^2 interaction t = 0.58, $P = 0.56$).

3.2 Multimodal fusion using linked ICA

The relative weight of modalities in each linked ICA output component is shown in **Figure 3**. Three components (IC10, IC14 and IC19) were excluded from further analysis as they were

dominated by signals from one or two subjects (e.g., due to regional hyperintensities reflected by ASL images). We focused on components with variance explained > 1%. Note that there was little fusion between functional signals and structural or vascular signals.

3.3 Relationship between age, gene group and neuroimaging components

Multiple regression analysis results of the linked ICA components of interest are shown in **Table 2**. We focused on components with a significant model fit (FDR-corrected $P < 0.05$ for adjusted R^2, i.e., the components that showed significant correlations with the variables being tested). Strong linear age effects were observed particularly in components indicating global CBF (IC1), ventral default mode network (IC5), salience network (IC7), and head motion (IC9) (**Figure 4**). Only one component, IC4, showed differential age effects between pre-symptomatic and non-carriers (Group:Age interaction t = -2.82, $P = 0.0051$). As age increases, pre-symptomatic genetic mutation carriers showed decreased activation of the left frontoparietal network (IC4, r = -0.30, $P < 0.001$), while non-carriers did not (r = -0.0087, $P = 0.91$). Brain visualization of IC4 and its scatter plot against age are shown in **Figure 5**.

Table 2. Multiple regression results of the linked independent component analysis components of interest (IC).

IC ~ Group*Age^2 + Gender + Total brain volume + Site															
		Model		**Group**		**Gender**		**Age**		**Age^2**		**Group:Age**		**Group:Age^2**	
IC	Variance explained	Adjusted R^2	*P*	β	*P*	β	*P*	β	*P*	β	*P*	β	*P*	β	*P*
IC1	14.23%	0.14	**< 0.001**	-0.17	**0.0048**	-0.26	**< 0.001**	-0.36	**< 0.001**	0.012	0.74	-0.011	0.82	-0.0032	0.93
IC2	9.81%	0.59	**< 0.001**	0.049	0.25	0.27	**< 0.001**	-0.082	**0.031**	-0.0085	0.74	0.036	0.29	-0.0049	0.85
IC3	6.56%	0.34	**< 0.001**	-0.080	0.14	0.090	0.075	-0.11	**0.022**	-0.029	0.38	-0.029	0.51	0.041	0.22
IC4	5.10%	0.27	**< 0.001**	-0.078	0.17	0.067	0.21	-0.13	**0.012**	0.032	0.36	-0.13	**0.0051**	0.034	0.33
IC5	4.09%	0.16	**< 0.001**	0.060	0.33	-0.052	0.36	-0.29	**< 0.001**	0.038	0.31	-0.092	0.062	-0.013	0.73
IC6	3.42%	0.12	**< 0.001**	-0.067	0.28	-0.16	**0.0067**	-0.15	**0.0058**	0.038	0.31	-0.084	0.10	0.068	0.077
IC7	2.18%	0.20	**< 0.001**	0.012	0.84	-0.024	0.66	-0.20	**< 0.001**	0.075	**0.040**	-0.085	0.075	0.028	0.44
IC8	1.91%	0.050	**0.013**	0.11	0.10	0.26	**< 0.001**	0.050	0.38	0.054	0.17	-0.039	0.45	-0.035	0.38
IC9	2.14%	0.47	**< 0.001**	-0.068	0.16	-0.62	**< 0.001**	-0.30	**< 0.001**	-0.049	0.10	0.025	0.53	0.032	0.28
IC12	2.13%	0.79	**< 0.001**	0.040	0.18	0.12	**< 0.001**	-0.017	0.53	-0.024	0.20	-0.0031	0.90	-0.026	0.17
IC13	1.02%	0.038	**0.039**	-0.036	0.58	-0.0081	0.89	0.072	0.22	-0.11	**0.0061**	-0.0035	0.95	0.022	0.58
IC15	2.63%	0.10	**< 0.001**	0.039	0.54	-0.12	**0.047**	0.0087	0.88	0.042	0.27	-0.048	0.35	0.0059	0.88
IC16	1.14%	0.28	**< 0.001**	0.031	0.59	-0.22	**< 0.001**	0.24	**< 0.001**	0.074	**0.032**	0.073	0.11	0.022	0.53
IC17	2.38%	0.33	**< 0.001**	-0.013	0.81	-0.12	**0.018**	-0.082	0.093	-0.0083	0.80	0.0092	0.84	-0.016	0.63
IC20	1.81%	0.063	**0.0032**	0.013	0.85	0.070	0.24	-0.10	0.10	0.029	0.46	-0.0016	0.98	-0.018	0.65
IC23	1.47%	0.053	**0.0096**	0.050	0.44	-0.050	0.41	0.053	0.36	-0.0083	0.83	-0.088	0.093	-0.030	0.45
IC26	1.59%	0.037	**0.043**	-0.012	0.85	0.22	**< 0.001**	0.075	0.20	-0.0034	0.93	-0.039	0.46	-0.015	0.70
IC29	1.45%	0.066	**0.0024**	0.025	0.70	0.046	0.44	0.12	**0.033**	0.066	0.10	0.017	0.74	0.042	0.28
IC31	1.22%	0.067	**0.0022**	0.0084	0.90	-0.10	0.10	-0.065	0.26	-0.067	0.090	-0.088	0.093	-0.00040	0.99
IC33	1.17%	0.039	**0.036**	-0.082	0.21	-0.021	0.73	0.0039	0.95	-0.052	0.20	-0.033	0.54	0.032	0.42

P values in bold are statistically significant

3.4. Relationship between neuroimaging components and cognitive function

All linked ICA components that showed cognition-related differences between the two groups reflected a single neuroimaging modality. No component showed a different association with cognition component 1 between non-carriers and pre-symptomatic carriers (**Supplementary Table**).

In regards to component 2 (**Supplementary Table**), IC2, indicating global GMV, showed an interaction with genetic mutation in predicting cognition component 2 (IC:Group t = -2.73, P = 0.0066): non-carriers showed a positive association between IC2 subject loadings and good performance on executive functions and poor performance on visuospatial memory tasks (r = 0.17, P = 0.026), while this association was not significant in pre-symptomatic carriers (r = -0.12, P = 0.10). There was a significant 3-way interaction between group, age and IC subject loadings of the left frontoparietal network (i.e., IC4, IC:Group:Age^2 t = -2.20, P = 0.029) in predicting cognition component 2. Visualizing the results (**Figure 6**) indicates that as age increased, an increased association between the left frontoparietal network and good performance on executive functions and poor performance on visuospatial memory tasks was found in pre-symptomatic genetic mutation carriers. This result was confirmed in a post-hoc test showing that a significant two-way interaction between IC4 and age in predicting these cognitive performances was found in pre-symptomatic genetic mutation carriers (IC:Age^2 t = -2.14, P = 0.033) but not in non-carriers (IC:Age^2 t = 1.70, P = 0.090). Significant 3-way interactions (IC:Group:Age^2) were also observed for the component of ventral default mode network (IC5, t = -2.73, P = 0.0068) and salience network (IC7, t = -3.14, P = 0.0018). The effects in both components suggested an

age-varying association between network activity and performance on executive functions in non-carriers but not in pre-symptomatic carriers (**Figure 6**).

4. Discussion

In this study, we co-analyzed grey matter volume, cerebral blood flow, and functional network integrity using a data-driven approach. Overall, the brain patterns and cognitive profiles of FTD genetic mutation carriers before symptom onset were very similar to controls without genetic mutations. However, this similarity diminishes as age increases. In particular, pre-symptomatic genetic mutation carriers showed a significant decrease in the left frontoparietal network integrity with age while non-carriers did not, suggesting a gene-related neurodegenerative consequence over and above normal ageing. The executive function of pre-symptomatic carriers dissociated from the level of atrophy if considered over all ages, but executive function became dependent on the left frontoparietal network integrity with age. This result is consistent with the hypothesis that maintaining integrity of the frontoparietal network might support cognitive function despite atrophy and hypoperfusion in pre-symptomatic FTD.

We confirmed the significant decreases with age in global CBF and ventral default mode network integrity. The decreases in CBF and default mode network activity are consistent with the commonly observed changes in perfusion [52, 53] and default mode network [54] in normal aging. We also demonstrated a significant decrease with age in global GMV, consistent with previous multimodal neuroimaging fusion studies [55-57] and normal aging pattern of the brain [58]. More importantly, we illustrated the age- and cognition-relevant divergence of frontoparietal network integrity between pre-symptomatic genetic mutation carriers and non-carriers. Pre-symptomatic genetic mutation carriers showed a significant decrease in the left frontoparietal network integrity with age while non-carriers did not. We suggest that the lateralized frontoparietal network is the functional network that is most affected by the effect of

FTD associated mutations with age. Reduced salience network connectivity is commonly observed in symptomatic bvFTD and associated with disease severity [46, 59]. However, in genetic mutation carriers before symptom onset, no significant alternation are observed in the salience network connectivity [60]. On the other hand, altered default mode network connectivity has been found in both pre-symptomatic *MAPT* mutation carriers and behavioral variant FTD subjects [46, 60]. In this study, we did not find the default mode network or the salience network significantly different between genetic mutation carriers and non-carriers when accounting for the age effects. Nevertheless, when relating to executive function, attention and processing speed, the associations between the ventral default mode network and the salience network, respectively, with performance on these functions were found particularly in younger non-carriers only but not in pre-symptomatic genetic mutation carriers, suggesting the cognitive reliance on these functional networks breaks down in genetic mutation carriers as well as during the ageing process. Understanding such an effect would be important for gaining insights into the mechanisms of cognitive decline and the maintenance of executive functions especially at the pre-symptomatic stage of cognitive impairment.

Although worse performance on some cognitive domains can be evident at the pre-symptomatic stage of FTD, in comparison with non-carrier controls [19, 21, 61], it is difficult to distinguish genetic mutation carriers from non-carriers simply based on performance on cognitive tasks. We found no significant difference in cognitive performance between genetic mutation carriers and non-carriers at the pre-symptomatic stage, confirming that genetic mutation carriers maintain similar overall cognition as non-carriers before symptom onset. However, we demonstrated that global cognition showed a trend of more rapid decline with age in pre-symptomatic genetic mutation carriers from the age of early 20s to 80s. It is important to note that between genetic

mutation carriers and non-carriers at the asymptomatic stage, brain characteristics such as GMV and frontoparietal functional network integrity were not differentially related to global cognitive performance but differentially related to executive functions, especially at older age. Maintenance of cognitive functions in genetic mutation carriers depends more on functional network integrity. This is consistent with findings from recent studies highlighting the link between functional networks and cognition in pre-symptomatic FTD [4, 10]. The performance related to attention, processing speed and executive functions was correlated with global GMV in non-carriers, while correlated with left frontoparietal network integrity in pre-symptomatic carriers especially as they get older. It suggests that in genetic mutation carriers, attention, processing speed and executive functions dissociated from GMV and were maintained by frontoparietal network integrity. Frontoparietal network is a large-scale network that has been suggested to be important for cognitive flexibility especially for executive function [62-64]. Executive function is one of the most commonly affected cognitive domains in FTD [1]. A recent study has found that *C9orf72* genetic mutation carriers showed lower attention and executive function at the pre-symptomatic stage compared to non-carriers [61]. Our study provides further evidence suggesting that these cognitive domains are sensitive to show alternations at the earlier stage of the disease. Given that CBF and GMV significantly decreased with age in all participants regardless of genetic mutations, and the reliance on other functional networks for cognitive performance broke down in genetic mutation carriers, maintaining frontoparietal network integrity might be the key to slowing cognitive decline at the pre-symptomatic stage of FTD, particularly slowing the decline in attention, processing speed and executive functions.

The strengths of this study include pathological confidence arising from genetic characterisation, and the large sample size of pre-symptomatic genetic mutation carriers through the multicentre GENFI study. Moreover, this study combines GMV, CBF and functional networks in genetic mutation carriers of FTD at the pre-symptomatic stage. It is important to link together neurobiological changes given the possible synergistic effects of multiple factors. Functional network connectivity and integrity may be related to other pathologies such as tau expression, amyloid load and changes in neurotransmitters in neurodegenerative diseases [46, 60, 65, 66]. Although we did not find an interplay among GMV, CBF and functional network integrity in pre-symptomatic mutation carriers, linking the frontoparietal network integrity to other pathologies that we have not yet explored in this study might be informative, given that the frontoparietal network was found to have age- and cognition-related distinction between pre-symptomatic mutation carriers and non-carriers.

This study also has limitations. First, due to the multicentre nature of the study, the variability of MRI acquisition scanners and sequences is higher than a single-centre study. However, we mitigated the effects through the use of the normalization approach and adjustment for site effects during preprocessing. Second, this study is cross-sectional. This should be noted when interpreting age effects, as dynamic ageing effects require longitudinal data. The recruitment and examination of the GENFI cohort are still ongoing. More follow-up visits in the future would allow a longitudinal examination of these participants, especially for the genetic mutation carriers that convert to symptomatic from pre-symptomatic. A longitudinal assessment could also include using baseline measures to predict future cognitive performance. Third, only adults were included in the study thus potentially missing the changes manifested before adulthood caused

by genetic mutation. A new cohort within GENFI is starting which aims to study family members below the age of 18.

In conclusion, we demonstrated that the frontoparietal network integrity of FTD genetic mutation carriers showed a distinctive relationship to age and cognitive function compared to non-carriers, before FTD symptom occurs. We suggest that the frontoparietal network integrity supports cognitive function in the presence of atrophy and hypoperfusion in pre-symptomatic FTD. While the linked ICA components indicating an interplay of brain structure, perfusion and functional network did not show differences related to genetic mutations, linking one or more of these neuroimaging biomarkers, especially functional network integrity, with other neuropathological changes is still a future direction for genetic FTD at the pre-symptomatic stage, which provides a window into the earliest possible stages of the disease. The dissociation of changes in structure blood flow and network activity in pre-symptomatic FTD has implications for clinical trials design, and strategies for prevention or treatments for people who are nominally well but at high risk of frontotemporal dementia.

References

[1] Bang J, Spina S, Miller BL. Frontotemporal dementia. Lancet. 2015;386:1672-82.

[2] Rohrer JD, Guerreiro R, Vandrovcova J, Uphill J, Reiman D, Beck J, et al. The heritability and genetics of frontotemporal lobar degeneration. Neurology. 2009;73:1451-6.

[3] Kinnunen KM, Cash DM, Poole T, Frost C, Benzinger TLS, Ahsan RL, et al. Presymptomatic atrophy in autosomal dominant Alzheimer's disease: A serial magnetic resonance imaging study. Alzheimers Dement. 2018;14:43-53.

[4] Tsvetanov KA, Gazzina S, Jones PS, van Swieten J, Borroni B, Sanchez-Valle R, et al. Brain functional network integrity sustains cognitive function despite atrophy in presymptomatic genetic frontotemporal dementia. Alzheimers Dement. 2021;17:500-14.

[5] Jack CR, Jr., Knopman DS, Jagust WJ, Shaw LM, Aisen PS, Weiner MW, et al. Hypothetical model of dynamic biomarkers of the Alzheimer's pathological cascade. Lancet Neurol. 2010;9:119-28.

[6] Rohrer JD, Nicholas JM, Cash DM, van Swieten J, Dopper E, Jiskoot L, et al. Presymptomatic cognitive and neuroanatomical changes in genetic frontotemporal dementia in the Genetic Frontotemporal dementia Initiative (GENFI) study: a cross-sectional analysis. Lancet Neurol. 2015;14:253-62.

[7] Cash DM, Bocchetta M, Thomas DL, Dick KM, van Swieten JC, Borroni B, et al. Patterns of gray matter atrophy in genetic frontotemporal dementia: results from the GENFI study. Neurobiology of Aging. 2018;62:191-6.

[8] Mutsaerts H, Mirza SS, Petr J, Thomas DL, Cash DM, Bocchetta M, et al. Cerebral perfusion changes in presymptomatic genetic frontotemporal dementia: a GENFI study. Brain. 2019;142:1108-20.

[9] Rittman T, Borchert R, Jones S, van Swieten J, Borroni B, Galimberti D, et al. Functional network resilience to pathology in presymptomatic genetic frontotemporal dementia. Neurobiol Aging. 2019;77:169-77.

[10] Whiteside DJ, Malpetti M, Jones PS, Ghosh BCP, Coyle-Gilchrist I, van Swieten JC, et al. Temporal dynamics predict symptom onset and cognitive decline in familial frontotemporal dementia. Alzheimers Dement. 2022.

[11] Miyagawa T, Brushaber D, Syrjanen J, Kremers W, Fields J, Forsberg LK, et al. Utility of the global CDR((R)) plus NACC FTLD rating and development of scoring rules: Data from the ARTFL/LEFFTDS Consortium. Alzheimers Dement. 2020;16:106-17.

[12] Gorno-Tempini ML, Hillis AE, Weintraub S, Kertesz A, Mendez M, Cappa SF, et al. Classification of primary progressive aphasia and its variants. Neurology. 2011;76:1006-14.

[13] Rascovsky K, Hodges JR, Knopman D, Mendez MF, Kramer JH, Neuhaus J, et al. Sensitivity of revised diagnostic criteria for the behavioural variant of frontotemporal dementia. Brain. 2011;134:2456-77.

[14] Mioshi E, Hsieh S, Savage S, Hornberger M, Hodges JR. Clinical staging and disease progression in frontotemporal dementia. Neurology. 2010;74:1591-7.

[15] Wear HJ, Wedderburn CJ, Mioshi E, Williams-Gray CH, Mason SL, Barker RA, Hodges JR. The Cambridge Behavioural Inventory revised. Dement Neuropsychol. 2008;2:102-7.

[16] Morris JC, Weintraub S, Chui HC, Cummings J, Decarli C, Ferris S, et al. The Uniform Data Set (UDS): clinical and cognitive variables and descriptive data from Alzheimer Disease Centers. Alzheimer Dis Assoc Disord. 2006;20:210-6.

[17] Corrigan JD, Hinkeldey NS. Relationships between parts A and B of the Trail Making Test. J Clin Psychol. 1987;43:402-9.
[18] Delis DC KE, Kramer J, den Buysch HO, Noens ILJ, Berckelaer-Onnes IA. DKEFS: Delis-Kaplan Executive Function System: Color-Word Interference Test: Handleiding: Pearson; 2008.
[19] Moore K, Convery R, Bocchetta M, Neason M, Cash DM, Greaves C, et al. A modified Camel and Cactus Test detects presymptomatic semantic impairment in genetic frontotemporal dementia within the GENFI cohort. Appl Neuropsychol Adult. 2022;29:112-9.
[20] Tombaugh TN, Kozak J, Rees L. Normative data stratified by age and education for two measures of verbal fluency: FAS and animal naming. Arch Clin Neuropsychol. 1999;14:167-77.
[21] Poos JM, Russell LL, Peakman G, Bocchetta M, Greaves CV, Jiskoot LC, et al. Impairment of episodic memory in genetic frontotemporal dementia: A GENFI study. Alzheimers Dement (Amst). 2021;13:e12185.
[22] Ashburner J. A fast diffeomorphic image registration algorithm. Neuroimage. 2007;38:95-113.
[23] Mutsaerts H, Petr J, Thomas DL, De Vita E, Cash DM, van Osch MJP, et al. Comparison of arterial spin labeling registration strategies in the multi-center GENetic frontotemporal dementia initiative (GENFI). J Magn Reson Imaging. 2018;47:131-40.
[24] Mutsaerts H, Petr J, Groot P, Vandemaele P, Ingala S, Robertson AD, et al. ExploreASL: An image processing pipeline for multi-center ASL perfusion MRI studies. Neuroimage. 2020;219:117031.
[25] Ashburner J, Friston KJ. Diffeomorphic registration using geodesic shooting and Gauss–Newton optimisation. NeuroImage. 2011;55:954-67.
[26] Shirzadi Z, Crane DE, Robertson AD, Maralani PJ, Aviv RI, Chappell MA, et al. Automated removal of spurious intermediate cerebral blood flow volumes improves image quality among older patients: A clinical arterial spin labeling investigation. Journal of Magnetic Resonance Imaging. 2015;42:1377-85.
[27] Alsop DC, Detre JA, Golay X, Günther M, Hendrikse J, Hernandez-Garcia L, et al. Recommended implementation of arterial spin-labeled perfusion MRI for clinical applications: A consensus of the ISMRM perfusion study group and the European consortium for ASL in dementia. Magnetic Resonance in Medicine. 2015;73:102-16.
[28] Asllani I, Borogovac A, Brown TR. Regression algorithm correcting for partial volume effects in arterial spin labeling MRI. Magnetic Resonance in Medicine. 2008;60:1362-71.
[29] Pasternak M MS, Luciw N, et al. Longitudinal cerebral perfusion in presymptomatic genetic frontotemporal dementia: GENFI results. Alzheimer's & Dementia. 2024;In-Press.
[30] Cusack R, Vicente-Grabovetsky A, Mitchell DJ, Wild CJ, Auer T, Linke AC, Peelle JE. Automatic analysis (aa): efficient neuroimaging workflows and parallel processing using Matlab and XML. Front Neuroinform. 2014;8:90.
[31] Pruim RHR, Mennes M, van Rooij D, Llera A, Buitelaar JK, Beckmann CF. ICA-AROMA: A robust ICA-based strategy for removing motion artifacts from fMRI data. Neuroimage. 2015;112:267-77.
[32] Pruim RHR, Mennes M, Buitelaar JK, Beckmann CF. Evaluation of ICA-AROMA and alternative strategies for motion artifact removal in resting state fMRI. Neuroimage. 2015;112:278-87.
[33] Geerligs L, Tsvetanov KA, Cam C, Henson RN. Challenges in measuring individual differences in functional connectivity using fMRI: The case of healthy aging. Hum Brain Mapp. 2017;38:4125-56.

[34] Calhoun VD, Adali T, Pearlson GD, Pekar JJ. A method for making group inferences from functional MRI data using independent component analysis. Hum Brain Mapp. 2001;14:140-51.
[35] Calhoun V. Data-driven approaches for identifying links between brain structure and function in health and disease. Dialogues Clin Neurosci. 2018;20:87-99.
[36] McKeown MJ, Makeig S, Brown GG, Jung TP, Kindermann SS, Bell AJ, Sejnowski TJ. Analysis of fMRI data by blind separation into independent spatial components. Hum Brain Mapp. 1998;6:160-88.
[37] Rosazza C, Minati L. Resting-state brain networks: literature review and clinical applications. Neurol Sci. 2011;32:773-85.
[38] Beckmann CF, DeLuca M, Devlin JT, Smith SM. Investigations into resting-state connectivity using independent component analysis. Philos Trans R Soc Lond B Biol Sci. 2005;360:1001-13.
[39] Damoiseaux JS, Rombouts SA, Barkhof F, Scheltens P, Stam CJ, Smith SM, Beckmann CF. Consistent resting-state networks across healthy subjects. Proc Natl Acad Sci U S A. 2006;103:13848-53.
[40] Smith SM, Fox PT, Miller KL, Glahn DC, Fox PM, Mackay CE, et al. Correspondence of the brain's functional architecture during activation and rest. Proc Natl Acad Sci U S A. 2009;106:13040-5.
[41] Himberg J, Hyvarinen A. Icasso: software for investigating the reliability of ICA estimates by clustering and visualization. 2003 IEEE XIII Workshop on Neural Networks for Signal Processing (IEEE Cat No03TH8718). 2003:259-68.
[42] Shirer WR, Ryali S, Rykhlevskaia E, Menon V, Greicius MD. Decoding subject-driven cognitive states with whole-brain connectivity patterns. Cereb Cortex. 2012;22:158-65.
[43] Tsvetanov KA, Henson RN, Tyler LK, Razi A, Geerligs L, Ham TE, et al. Extrinsic and Intrinsic Brain Network Connectivity Maintains Cognition across the Lifespan Despite Accelerated Decay of Regional Brain Activation. J Neurosci. 2016;36:3115-26.
[44] Liu X, Tyler LK, Cam CAN, Rowe JB, Tsvetanov KA. Multimodal fusion analysis of functional, cerebrovascular and structural neuroimaging in healthy aging subjects. Hum Brain Mapp. 2022.
[45] Passamonti L, Tsvetanov KA, Jones PS, Bevan-Jones WR, Arnold R, Borchert RJ, et al. Neuroinflammation and Functional Connectivity in Alzheimer's Disease: Interactive Influences on Cognitive Performance. The Journal of Neuroscience. 2019;39:7218-26.
[46] Pievani M, de Haan W, Wu T, Seeley WW, Frisoni GB. Functional network disruption in the degenerative dementias. Lancet Neurol. 2011;10:829-43.
[47] Snyder W, Uddin LQ, Nomi JS. Dynamic functional connectivity profile of the salience network across the life span. Hum Brain Mapp. 2021;42:4740-9.
[48] Groves AR, Beckmann CF, Smith SM, Woolrich MW. Linked independent component analysis for multimodal data fusion. Neuroimage. 2011;54:2198-217.
[49] Smith SM, Jenkinson M, Woolrich MW, Beckmann CF, Behrens TE, Johansen-Berg H, et al. Advances in functional and structural MR image analysis and implementation as FSL. Neuroimage. 2004;23 Suppl 1:S208-19.
[50] Groves AR, Smith SM, Fjell AM, Tamnes CK, Walhovd KB, Douaud G, et al. Benefits of multi-modal fusion analysis on a large-scale dataset: life-span patterns of inter-subject variability in cortical morphometry and white matter microstructure. Neuroimage. 2012;63:365-80.
[51] Wilkinson GN, Rogers CE. Symbolic Description of Factorial Models for Analysis of Variance. Journal of the Royal Statistical Society Series C (Applied Statistics). 1973;22:392-9.

[52] Zhang N, Gordon ML, Goldberg TE. Cerebral blood flow measured by arterial spin labeling MRI at resting state in normal aging and Alzheimer's disease. Neurosci Biobehav Rev. 2017;72:168-75.
[53] Mokhber N, Shariatzadeh A, Avan A, Saber H, Babaei GS, Chaimowitz G, Azarpazhooh MR. Cerebral blood flow changes during aging process and in cognitive disorders: A review. Neuroradiol J. 2021;34:300-7.
[54] Damoiseaux JS, Beckmann CF, Arigita EJ, Barkhof F, Scheltens P, Stam CJ, et al. Reduced resting-state brain activity in the "default network" in normal aging. Cereb Cortex. 2008;18:1856-64.
[55] Doan NT, Engvig A, Zaske K, Persson K, Lund MJ, Kaufmann T, et al. Distinguishing early and late brain aging from the Alzheimer's disease spectrum: consistent morphological patterns across independent samples. Neuroimage. 2017;158:282-95.
[56] Douaud G, Groves AR, Tamnes CK, Westlye LT, Duff EP, Engvig A, et al. A common brain network links development, aging, and vulnerability to disease. Proc Natl Acad Sci U S A. 2014;111:17648-53.
[57] Liu X, Tyler LK, Cam CAN, Rowe JB, Tsvetanov KA. Multimodal fusion analysis of functional, cerebrovascular and structural neuroimaging in healthy aging subjects. Hum Brain Mapp. 2022;43:5490-508.
[58] Kennedy KM, Raz N. Normal Aging of the Brain. In: Toga AW, editor. Brain Mapping. Waltham: Academic Press; 2015. p. 603-17.
[59] Zhou J, Greicius MD, Gennatas ED, Growdon ME, Jang JY, Rabinovici GD, et al. Divergent network connectivity changes in behavioural variant frontotemporal dementia and Alzheimer’s disease. Brain. 2010;133:1352-67.
[60] Whitwell JL, Josephs KA, Avula R, Tosakulwong N, Weigand SD, Senjem ML, et al. Altered functional connectivity in asymptomatic MAPT subjects: a comparison to bvFTD. Neurology. 2011;77:866-74.
[61] Poos JM, MacDougall A, van den Berg E, Jiskoot LC, Papma JM, van der Ende EL, et al. Longitudinal Cognitive Changes in Genetic Frontotemporal Dementia Within the GENFI Cohort. Neurology. 2022;99:e281-e95.
[62] Kupis L, Goodman ZT, Kornfeld S, Hoang S, Romero C, Dirks B, et al. Brain Dynamics Underlying Cognitive Flexibility Across the Lifespan. Cereb Cortex. 2021;31:5263-74.
[63] Adnan A, Beaty R, Lam J, Spreng RN, Turner GR. Intrinsic default-executive coupling of the creative aging brain. Soc Cogn Affect Neurosci. 2019;14:291-303.
[64] Qin J, Chen SG, Hu D, Zeng LL, Fan YM, Chen XP, Shen H. Predicting individual brain maturity using dynamic functional connectivity. Front Hum Neurosci. 2015;9:418.
[65] Murley AG, Rowe JB. Neurotransmitter deficits from frontotemporal lobar degeneration. Brain. 2018;141:1263-85.
[66] Hedden T, Van Dijk KR, Becker JA, Mehta A, Sperling RA, Johnson KA, Buckner RL. Disruption of functional connectivity in clinically normal older adults harboring amyloid burden. J Neurosci. 2009;29:12686-94.

Consent Statement

All participants provided informed consent.

Acknowledgements

X.L. is supported by the Cambridge Commonwealth, European and International Trust. J.C.V.S., L.C.J. and H.S. are supported by the Dioraphte Foundation grant 09-02-03-00, Association for Frontotemporal Dementias Research Grant 2009, Netherlands Organization for Scientific Research grant HCMI 056-13-018, ZonMw Memorabel (Deltaplan Dementie, project number 733 051 042), ZonMw Onderzoeksprogramma Dementie (YOD-INCLUDED, project number10510032120002), EU Joint Programme-Neurodegenerative Disease Research-GENFI-PROX, Alzheimer Nederland and the Bluefield Project. R.S-V. is supported by Alzheimer's Research UK Clinical Research Training Fellowship (ARUK-CRF2017B-2) and has received funding from Fundació Marató de TV3, Spain (grant no. 20143810). C.G. received funding from EU Joint Programme-Neurodegenerative Disease Research-Prefrontals Vetenskapsrådet Dnr 529-2014-7504, EU Joint Programme-Neurodegenerative Disease Research-GENFI-PROX, Vetenskapsrådet 2019-0224, Vetenskapsrådet 2015-02926, Vetenskapsrådet 2018-02754, the Swedish FTD Inititative-Schörling Foundation, Alzheimer Foundation, Brain Foundation, Dementia Foundation and Region Stockholm ALF-project. D.G. received support from the EU Joint Programme-Neurodegenerative Disease Research and the Italian Ministry of Health (PreFrontALS) grant 733051042. R.V. has received funding from the Mady Browaeys Fund for Research into Frontotemporal Dementia. J.L. received funding for this work by the Deutsche Forschungsgemeinschaft German Research Foundation under Germany's Excellence Strategy within the framework of the Munich Cluster for Systems Neurology (EXC 2145 SyNergy—ID 390857198). M.O. has received funding from Germany's Federal Ministry of Education and Research (BMBF). E.F. has received funding from a Canadian Institute of Health Research grant #327387. M.M. has received funding from a Canadian Institute of Health Research operating grant and the Weston Brain Institute and Ontario Brain Institute. F.M. is supported by the Tau Consortium and has received funding from the Carlos III Health Institute (PI19/01637). J.D.R. is supported by the Bluefield Project and the National Institute for Health and Care Research University College London Hospitals Biomedical Research Centre, and has received funding from an MRC Clinician Scientist Fellowship (MR/M008525/1) and a Miriam Marks Brain Research UK Senior Fellowship. Several authors of this publication (J.C.V.S., M.S., R.V., A.d.M., M.O., R.V., J.D.R.) are members of the European Reference Network for Rare Neurological Diseases (ERN-RND) - Project ID No 739510. K.A.T. was supported by the Guarantors of Brain (G101149) and Alzheimer's Society (Grant Nr. 602). J.B.R. has received funding from the Welcome Trust (103838; 220258) and is supported by the Cambridge University Centre for Frontotemporal Dementia, the Medical Research Council (MC_UU_00030/14; MR/T033371/1) and the National Institute for Health Research Cambridge Biomedical Research Centre (NIHR203312: BRC-1215-20014) and the Holt Fellowship. This work was also supported by the EU Joint Programme-Neurodegenerative Disease Research GENFI-PROX grant [2019-02248; to J.D.R., M.O., B.B., C.G., J.C.V.S. and M.S. For the purpose of open access, the author has applied a CC BY public copyright licence to any Author Accepted Manuscript version arising from this submission.

Conflict of Interest

James B. Rowe is a non-remunerated trustee of the Guarantors of Brain, Darwin College, and the PSP Association; he provides consultancy to Alzheimer Research UK, Asceneuron, Alector, Biogen, CuraSen, CumulusNeuro, UCB, SV Health, and Wave, and has research grants from AZ-Medimmune, Janssen, Lilly as industry partners in the Dementias Platform UK.

Keywords

multimodal neuroimaging, frontotemporal dementia, functional network, cerebral blood flow, atrophy, pre-symptomatic dementia

The GENFI Consortium Author List

Rhian Convery	Department of Neurodegenerative Disease, Dementia Research Centre, UCL Queen Square Institute of Neurology, London, UK
Martina Bocchetta	Department of Neurodegenerative Disease, Dementia Research Centre, UCL Queen Square Institute of Neurology, London, UK
David Cash	Department of Neurodegenerative Disease, Dementia Research Centre, UCL Queen Square Institute of Neurology, London, UK
Sophie Goldsmith	Department of Neurodegenerative Disease, Dementia Research Centre, UCL Queen Square Institute of Neurology, London, UK
Kiran Samra	Department of Neurodegenerative Disease, Dementia Research Centre, UCL Queen Square Institute of Neurology, London, UK
David L. Thomas	Neuroimaging Analysis Centre, Department of Brain Repair and Rehabilitation, UCL Institute of Neurology, Queen Square, London, UK
Thomas Cope	Cambridge University Hospitals NHS Trust, University of Cambridge, Cambridge, UK
Timothy Rittman	Department of Clinical Neurosciences, University of Cambridge, Cambridge, UK
Antonella Alberici	Centre for Neurodegenerative Disorders, Department of Clinical and Experimental Sciences, University of Brescia, Brescia, Italy
Enrico Premi	Stroke Unit, ASST Brescia Hospital, Brescia, Italy
Roberto Gasparotti	Neuroradiology Unit, University of Brescia, Brescia, Italy
Emanuele Buratti	ICGEB Trieste, Italy
Valentina Cantoni	Centre for Neurodegenerative Disorders, Department of Clinical and Experimental Sciences, University of Brescia, Brescia, Italy
Andrea Arighi	Fondazione IRCCS Ca' Granda Ospedale Maggiore Policlinico, Neurodegenerative Diseases Unit, Milan, Italy
Chiara Fenoglio	University of Milan, Centro Dino Ferrari, Milan, Italy
Vittoria Borracci	Fondazione IRCCS Ca' Granda Ospedale Maggiore Policlinico, Neurodegenerative Diseases Unit, Milan, Italy

Maria Serpente	Fondazione IRCCS Ca' Granda Ospedale Maggiore Policlinico, Neurodegenerative Diseases Unit, Milan, Italy
Tiziana Carandini	Fondazione IRCCS Ca' Granda Ospedale Maggiore Policlinico, Neurodegenerative Diseases Unit, Milan, Italy
Emanuela Rotondo	Fondazione IRCCS Ca' Granda Ospedale Maggiore Policlinico, Neurodegenerative Diseases Unit, Milan, Italy
Giacomina Rossi	Fondazione IRCCS Istituto Neurologico Carlo Besta, Milano, Italy
Giorgio Giaccone	Fondazione IRCCS Istituto Neurologico Carlo Besta, Milano, Italy
Giuseppe Di Fede	Fondazione IRCCS Istituto Neurologico Carlo Besta, Milano, Italy
Paola Caroppo	Fondazione IRCCS Istituto Neurologico Carlo Besta, Milano, Italy
Sara Prioni	Fondazione IRCCS Istituto Neurologico Carlo Besta, Milano, Italy
Veronica Redaelli	Fondazione IRCCS Istituto Neurologico Carlo Besta, Milano, Italy
David Tang-Wai	The University Health Network, Krembil Research Institute, Toronto, Canada
Ekaterina Rogaeva	Tanz Centre for Research in Neurodegenerative Diseases, University of Toronto, Toronto, Canada
Miguel Castelo-Branco	Faculty of Medicine, ICNAS, CIBIT, University of Coimbra, Coimbra, Portugal.
Morris Freedman	Baycrest Health Sciences, Rotman Research Institute, University of Toronto, Toronto, Canada
Ron Keren	The University Health Network, Toronto Rehabilitation Institute, Toronto, Canada
Sandra Black	Sunnybrook Health Sciences Centre, Sunnybrook Research Institute, University of Toronto, Toronto, Canada
Sara Mitchell	Sunnybrook Health Sciences Centre, Sunnybrook Research Institute, University of Toronto, Toronto, Canada
Christen Shoesmith	Department of Clinical Neurological Sciences, University of Western Ontario, London, Ontario, Canada
Robart Bartha	Department of Medical Biophysics, The University of Western Ontario, London, Ontario, Canada; Centre for Functional and Metabolic Mapping, Robarts Research Institute, The University of Western Ontario, London, Ontario, Canada
Rosa Rademakers	Center for Molecular Neurology, University of Antwerp
Jackie Poos	Department of Neurology, Erasmus Medical Center, Rotterdam, Netherlands
Janne M. Papma	Department of Neurology, Erasmus Medical Center, Rotterdam, Netherlands
Lucia Giannini	Department of Neurology, Erasmus Medical Center, Rotterdam, Netherlands
Liset de Boer	Department of Neurology, Erasmus Medical Center, Rotterdam, Netherlands

Julie de Houwer	Department of Neurology, Erasmus Medical Center, Rotterdam, Netherlands
Rick van Minkelen	Department of Clinical Genetics, Erasmus Medical Center, Rotterdam, Netherlands
Yolande Pijnenburg	Amsterdam University Medical Centre, Amsterdam VUmc, Amsterdam, Netherlands
Benedetta Nacmias	Department of Neuroscience, Psychology, Drug Research and Child Health, University of Florence, Florence, Italy
Camilla Ferrari	Department of Neuroscience, Psychology, Drug Research and Child Health, University of Florence, Florence, Italy
Cristina Polito	Department of Biomedical, Experimental and Clinical Sciences "Mario Serio", Nuclear Medicine Unit, University of Florence, Florence, Italy
Gemma Lombardi	Department of Neuroscience, Psychology, Drug Research and Child Health, University of Florence, Florence, Italy
Valentina Bessi	Department of Neuroscience, Psychology, Drug Research and Child Health, University of Florence, Florence, Italy
Mattias Nilsson	Department of Clinical Neuroscience, Karolinska Institutet, Stockholm, Sweden
Henrik Viklund	Karolinska University Hospital Huddinge
Melissa Taheri Rydell	Department of Neurobiology, Care Sciences and Society; Center for Alzheimer Research, Division of Neurogeriatrics, , Bioclinicum, Karolinska Institutet, Solna, Sweden; Unit for Hereditary Dementias, Theme inflammation and Aging, Karolinska University Hospital, Solna, Sweden
Vesna Jelic	Department of Neurobiology, Care Sciences and Society; Division of Clinical Geriatrics, Karolinska Institutet, Stockholm, Sweden; Cognitive clinic, Theme inflammation and Aging, Karolinska University Hospital, Solna, Sweden
Linn Öijerstedt	Department of Neurobiology, Care Sciences and Society; Center for Alzheimer Research, Division of Neurogeriatrics, , Bioclinicum, Karolinska Institutet, Solna, Sweden; Unit for Hereditary Dementias, Theme inflammation and Aging, Karolinska University Hospital, Solna, Sweden
Tobias Langheinrich	Division of Neuroscience and Experimental Psychology, Wolfson Molecular Imaging Centre, University of Manchester, Manchester, UK; Manchester Centre for Clinical Neurosciences, Department of Neurology, Salford Royal NHS Foundation Trust, Manchester, UK
Albert Lladó	Alzheimer's disease and Other Cognitive Disorders Unit, Neurology Service, Hospital Clínic, Barcelona, Spain
Anna Antonell	Alzheimer's disease and Other Cognitive Disorders Unit, Neurology Service, Hospital Clínic, Barcelona, Spain
Jaume Olives	Alzheimer's disease and Other Cognitive Disorders Unit, Neurology Service, Hospital Clínic, Barcelona, Spain
Mircea Balasa	Alzheimer's disease and Other Cognitive Disorders Unit, Neurology Service, Hospital Clínic, Barcelona, Spain
Nuria Bargalló	Imaging Diagnostic Center, Hospital Clínic, Barcelona, Spain
Sergi	Alzheimer's disease and Other Cognitive Disorders Unit, Neurology Service,

Borrego-Ecija	Hospital Clínic, Barcelona, Spain
Ana Verdelho	Department of Neurosciences and Mental Health, Centro Hospitalar Lisboa Norte - Hospital de Santa Maria & Faculty of Medicine, University of Lisbon, Lisbon, Portugal
Carolina Maruta	Laboratory of Language Research, Centro de Estudos Egas Moniz, Faculty of Medicine, University of Lisbon, Lisbon, Portugal
Tiago Coelho	Faculty of Medicine, University of Lisbon, Lisbon, Portugal
Gabriel Miltenberger	Faculty of Medicine, University of Lisbon, Lisbon, Portugal
Frederico Simões do Couto	Faculdade de Medicina, Universidade Católica Portuguesa
Alazne Gabilondo	Cognitive Disorders Unit, Department of Neurology, Donostia University Hospital, San Sebastian, Gipuzkoa, Spain; Neuroscience Area, Biodonostia Health Research Insitute, San Sebastian, Gipuzkoa, Spain
Ioana Croitoru	Neuroscience Area, Biodonostia Health Research Insitute, San Sebastian, Gipuzkoa, Spain
Mikel Tainta	Neuroscience Area, Biodonostia Health Research Insitute, San Sebastian, Gipuzkoa, Spain
Myriam Barandiaran	Cognitive Disorders Unit, Department of Neurology, Donostia University Hospital, San Sebastian, Gipuzkoa, Spain; Neuroscience Area, Biodonostia Health Research Insitute, San Sebastian, Gipuzkoa, Spain
Patricia Alves	Neuroscience Area, Biodonostia Health Research Insitute, San Sebastian, Gipuzkoa, Spain; Department of Educational Psychology and Psychobiology, Faculty of Education, International University of La Rioja, Logroño, Spain
Benjamin Bender	Department of Diagnostic and Interventional Neuroradiology, University of Tübingen, Tübingen, Germany
David Mengel	Department of Neurodegenerative Diseases, Hertie-Institute for Clinical Brain Research and Center of Neurology, University of Tübingen, Tübingen, Germany; Center for Neurodegenerative Diseases (DZNE), Tübingen, Germany
Lisa Graf	Department of Neurodegenerative Diseases, Hertie-Institute for Clinical Brain Research and Center of Neurology, University of Tübingen, Tübingen, Germany
Annick Vogels	Department of Human Genetics, KU Leuven, Leuven, Belgium
Mathieu Vandenbulcke	Geriatric Psychiatry Service, University Hospitals Leuven, Belgium; Neuropsychiatry, Department of Neurosciences, KU Leuven, Leuven, Belgium
Philip Van Damme	Neurology Service, University Hospitals Leuven, Belgium; Laboratory for Neurobiology, VIB-KU Leuven Centre for Brain Research, Leuven, Belgium
Rose Bruffaerts	Department of Biomedical Sciences, University of Antwerp, Antwerp, Belgium; Biomedical Research Institute, Hasselt University, 3500 Hasselt, Belgium
Koen Poesen	Laboratory for Molecular Neurobiomarker Research, KU Leuven, Leuven, Belgium
Pedro Rosa-	Translational Neuroimaging Laboratory, McGill Centre for Studies in Aging,

Neto	McGill University, Montreal, Québec, Canada
Maxime Montembault	Douglas Research Centre, Department of Psychiatry, McGill University, Montreal, Québec, Canada
Agnès Camuzat	Sorbonne Université, Paris Brain Institute – Institut du Cerveau – ICM, Inserm U1127, CNRS UMR 7225, AP-HP - Hôpital Pitié-Salpêtrière, Paris, France
Alexis Brice	Sorbonne Université, Paris Brain Institute – Institut du Cerveau – ICM, Inserm U1127, CNRS UMR 7225, AP-HP - Hôpital Pitié-Salpêtrière, Paris, France; Reference Network for Rare Neurological Diseases (ERN-RND)
Anne Bertrand	Sorbonne Université, Paris Brain Institute – Institut du Cerveau – ICM, Inserm U1127, CNRS UMR 7225, AP-HP - Hôpital Pitié-Salpêtrière, Paris, France; Inria, Aramis project-team, F-75013, Paris, France; Centre pour l'Acquisition et le Traitement des Images, Institut du Cerveau et la Moelle, Paris, France
Aurélie Funkiewiez	Sorbonne Université, Paris Brain Institute – Institut du Cerveau – ICM, Inserm U1127, CNRS UMR 7225, AP-HP - Hôpital Pitié-Salpêtrière, Paris, France; Centre de référence des démences rares ou précoces, IM2A, Département de Neurologie, AP-HP - Hôpital Pitié-Salpêtrière, Paris, France
Daisy Rinaldi	Sorbonne Université, Paris Brain Institute – Institut du Cerveau – ICM, Inserm U1127, CNRS UMR 7225, AP-HP - Hôpital Pitié-Salpêtrière, Paris, France; Centre de référence des démences rares ou précoces, IM2A, Département de Neurologie, AP-HP - Hôpital Pitié-Salpêtrière, Paris, France; Département de Neurologie, AP-HP - Hôpital Pitié-Salpêtrière, Paris, France
Dario Saracino	Sorbonne Université, Paris Brain Institute – Institut du Cerveau – ICM, Inserm U1127, CNRS UMR 7225, AP-HP - Hôpital Pitié-Salpêtrière, Paris, France; Centre de référence des démences rares ou précoces, IM2A, Département de Neurologie, AP-HP - Hôpital Pitié-Salpêtrière, Paris, France; Inria, Aramis project-team, F-75013, Paris, France
Olivier Colliot	Sorbonne Université, Paris Brain Institute – Institut du Cerveau – ICM, Inserm U1127, CNRS UMR 7225, AP-HP - Hôpital Pitié-Salpêtrière, Paris, France; Centre pour l'Acquisition et le Traitement des Images, Institut du Cerveau et la Moelle, Paris, France; Inria, Aramis project-team, F-75013, Paris, France
Sabrina Sayah	Sorbonne Université, Paris Brain Institute – Institut du Cerveau – ICM, Inserm U1127, CNRS UMR 7225, AP-HP - Hôpital Pitié-Salpêtrière, Paris, France
Catharina Prix	Neurologische Klinik, Ludwig-Maximilians-Universität München, Munich, Germany
Elisabeth Wlasich	Neurologische Klinik, Ludwig-Maximilians-Universität München, Munich, Germany
Olivia Wagemann	Neurologische Klinik, Ludwig-Maximilians-Universität München, Munich, Germany
Sonja Schönecker	Neurologische Klinik, Ludwig-Maximilians-Universität München, Munich, Germany
Alexander Maximilian Bernhardt	Neurologische Klinik, Ludwig-Maximilians-Universität München, Munich, Germany
Anna Stockbauer	Neurologische Klinik, Ludwig-Maximilians-Universität München, Munich, Germany

Jolina Lombardi	Department of Neurology, University of Ulm, Ulm
Sarah Anderl-Straub	Department of Neurology, University of Ulm, Ulm, Germany
Adeline Rollin	CHU, CNR-MAJ, Labex Distalz, LiCEND Lille, France
Gregory Kuchcinski	Univ Lille, France; Inserm 1172, Lille, France; CHU, CNR-MAJ, Labex Distalz, LiCEND Lille, France
Maxime Bertoux	Inserm 1172, Lille, France; CHU, CNR-MAJ, Labex Distalz, LiCEND Lille, France
Thibaud Lebouvier	Univ Lille, France; Inserm 1172, Lille, France; CHU, CNR-MAJ, Labex Distalz, LiCEND Lille, France
Vincent Deramecourt	Univ Lille, France; Inserm 1172, Lille, France; CHU, CNR-MAJ, Labex Distalz, LiCEND Lille, France
João Durães	Neurology Department, Centro Hospitalar e Universitario de Coimbra, Coimbra, Portugal
Marisa Lima	Neurology Department, Centro Hospitalar e Universitario de Coimbra, Coimbra, Portugal
Maria João Leitão	Centre of Neurosciences and Cell Biology, Universidade de Coimbra, Coimbra, Portugal
Maria Rosario Almeida	Faculty of Medicine, University of Coimbra, Coimbra, Portugal
Miguel Tábuas-Pereira	Neurology Department, Centro Hospitalar e Universitario de Coimbra, Coimbra, Portugal; Faculty of Medicine, University of Coimbra, Coimbra, Portugal.
Sónia Afonso	Instituto Ciencias Nucleares Aplicadas a Saude, Universidade de Coimbra, Coimbra, Portugal
João Lemos	Faculty of Medicine, University of Coimbra, Coimbra, Portugal

691 **Figure Captions**
692

693 **Figure 1**. Summary of processing and analysis of the imaging modalities, comprising functional,
694 cerebrovascular, and structural measurements. CBF, cerebral blood flow; DMN, default mode
695 network; FPN, frontoparietal network; GMV, grey matter volume; ICA, independent component
696 analysis; fMRI, functional magnetic resonance imaging; SN, salience network; T1w, T1-weighted.

697 **Figure 2**. The two significant components from principal component analysis (PCA) on cognitive
698 assessments. The top row shows the loadings of each cognitive test in PCA components. The
699 bottom row shows the scatter plots of the correlation between age and PCA cognition
700 component scores.

701 **Figure 3**. The relative weight of modalities in each component generated from linked
702 independent component analysis (ICA) and the percentage of variance explained of each
703 component. CBF, cerebral blood flow; dDMN, dorsal default mode network; vDMN, ventral
704 default mode network; FPN, frontoparietal network; GMV, grey matter volume; SN, salience
705 network.

706 **Figure 4**. Brain visualization and scatter plots of subject loadings against age of the linked
707 independent component analysis components (ICs) showing strong age effects.

708 **Figure 5**. Brain visualization of linked independent component analysis component 4 (IC4),
709 showing the left frontoparietal network (FPN). For visualization, the brain spatial map threshold
710 is set to $3 < |Z| < 10$. The scatter plot shows the correlation between age and IC4 subject
711 loadings, separated by pre-symptomatic genetic mutation carriers ($r = -0.30$, $P < 0.001$) and
712 non-carriers ($r = -0.0087$, $P = 0.91$).

713 **Figure 6**. Linked independent component analysis components showing three-way interactions
714 between subject loadings with group (genetic mutation) and age in predicting cognition
715 component 2. IC4 indicates the left frontoparietal network (FPN), IC5 indicates the ventral
716 default mode network (DMN), and IC7 indicates the salience network (SN). The brain
717 visualization and scatter plots are shown. The scatter plots show the correlation between IC
718 subject loading scores and PCA cognition component 2 scores, for visualization purpose
719 separated by pre-symptomatic genetic mutation carriers and non-carriers and three age groups.

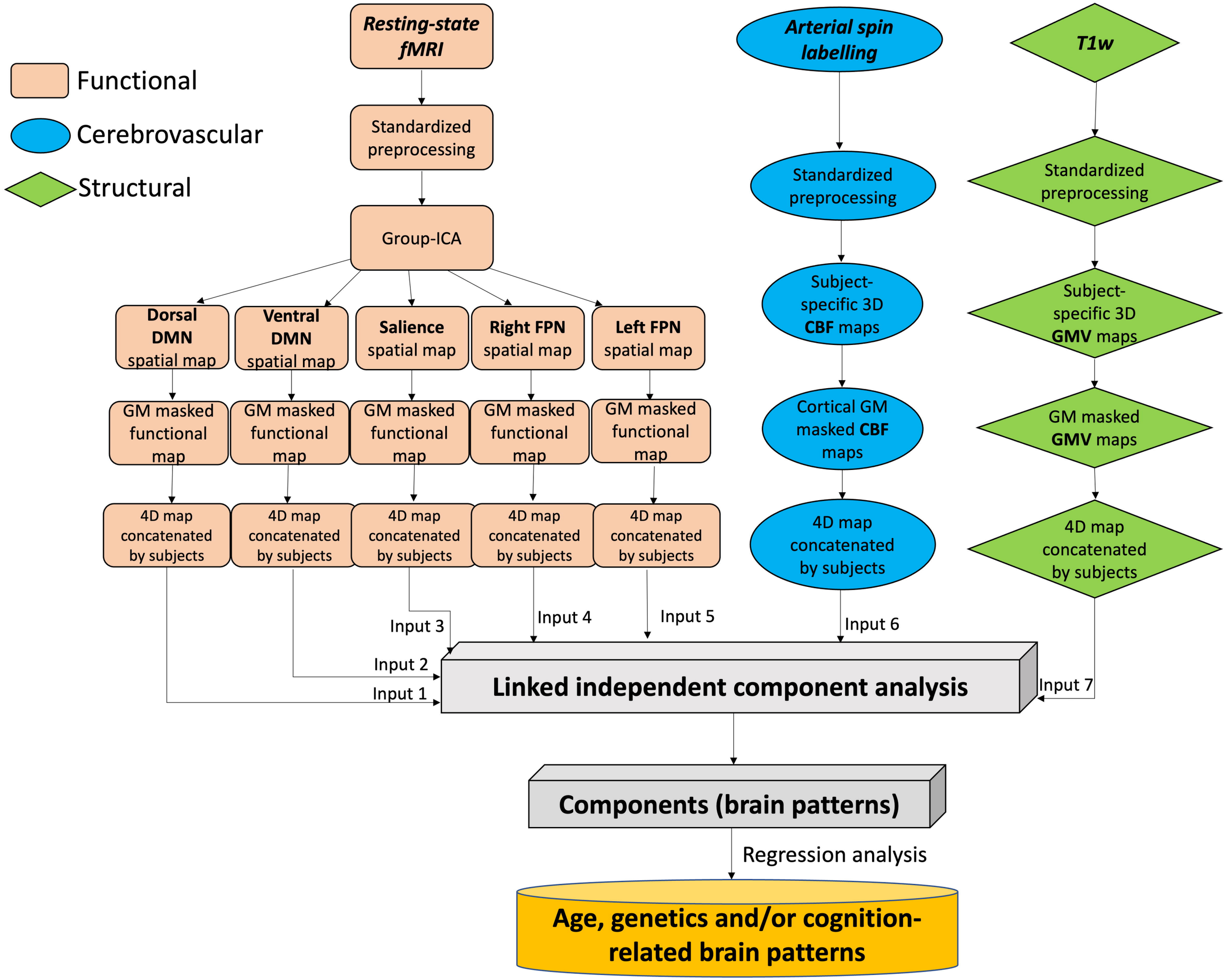
Functional
Cerebrovascular
Structural
Resting-state fMRI
Standardized preprocessing
Group-ICA
Dorsal DMN spatial map
Ventral DMN spatial map
Salience spatial map
Right FPN spatial map
Left FPN spatial map
GM masked functional map
4D map concatenated by subjects
Arterial spin labelling
Standardized preprocessing
Subject-specific 3D CBF maps
Cortical GM masked CBF maps
4D map concatenated by subjects
T1w
Standardized preprocessing
Subject-specific 3D GMV maps
GM masked GMV maps
4D map concatenated by subjects
Input 1
Input 2
Input 3
Input 4
Input 5
Input 6
Input 7
Linked independent component analysis
Components (brain patterns)
Regression analysis
Age, genetics and/or cognition-related brain patterns

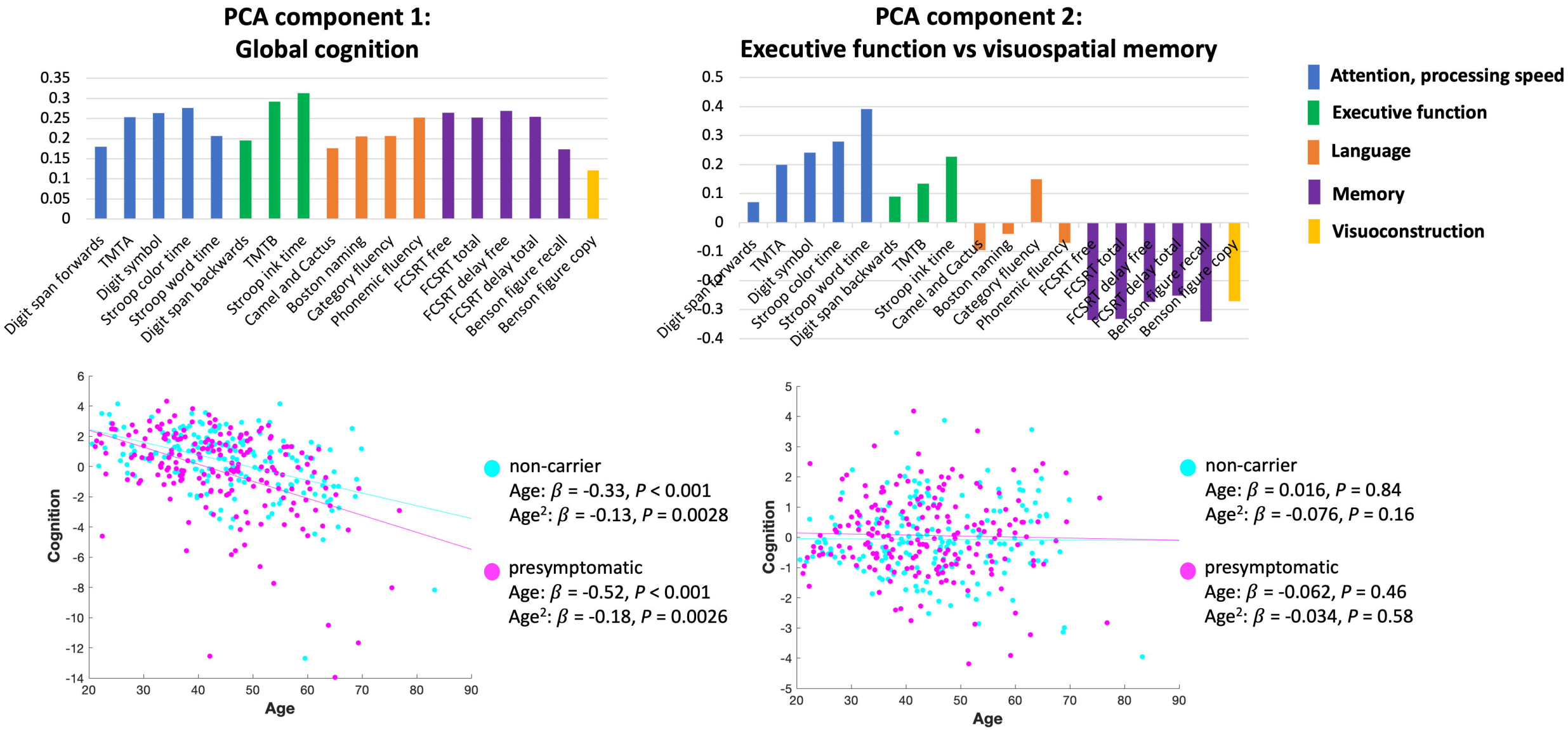
PCA component 1:
Global cognition
0.35
0.3
0.25
0.2
0.15
0.1
0.05
0
Digit span forwards
TMTA
Digit symbol
Stroop color time
Stroop word time
Digit span backwards
TMTB
Stroop ink time
Camel and Cactus
Boston naming
Category fluency
Phonemic fluency
FCSRT free
FCSRT total
FCSRT delay free
FCSRT delay total
Benson figure recall
Benson figure copy
PCA component 2:
Executive function vs visuospatial memory
0.5
0.4
0.3
0.2
0.1
0
-0.1
-0.2
-0.3
-0.4
Attention, processing speed
Executive function
Language
Memory
Visuoconstruction
Cognition
Age
non-carrier
Age: β = -0.33, P < 0.001
Age²: β = -0.13, P = 0.0028
presymptomatic
Age: β = -0.52, P < 0.001
Age²: β = -0.18, P = 0.0026
Cognition
Age
non-carrier
Age: β = 0.016, P = 0.84
Age²: β = -0.076, P = 0.16
presymptomatic
Age: β = -0.062, P = 0.46
Age²: β = -0.034, P = 0.58

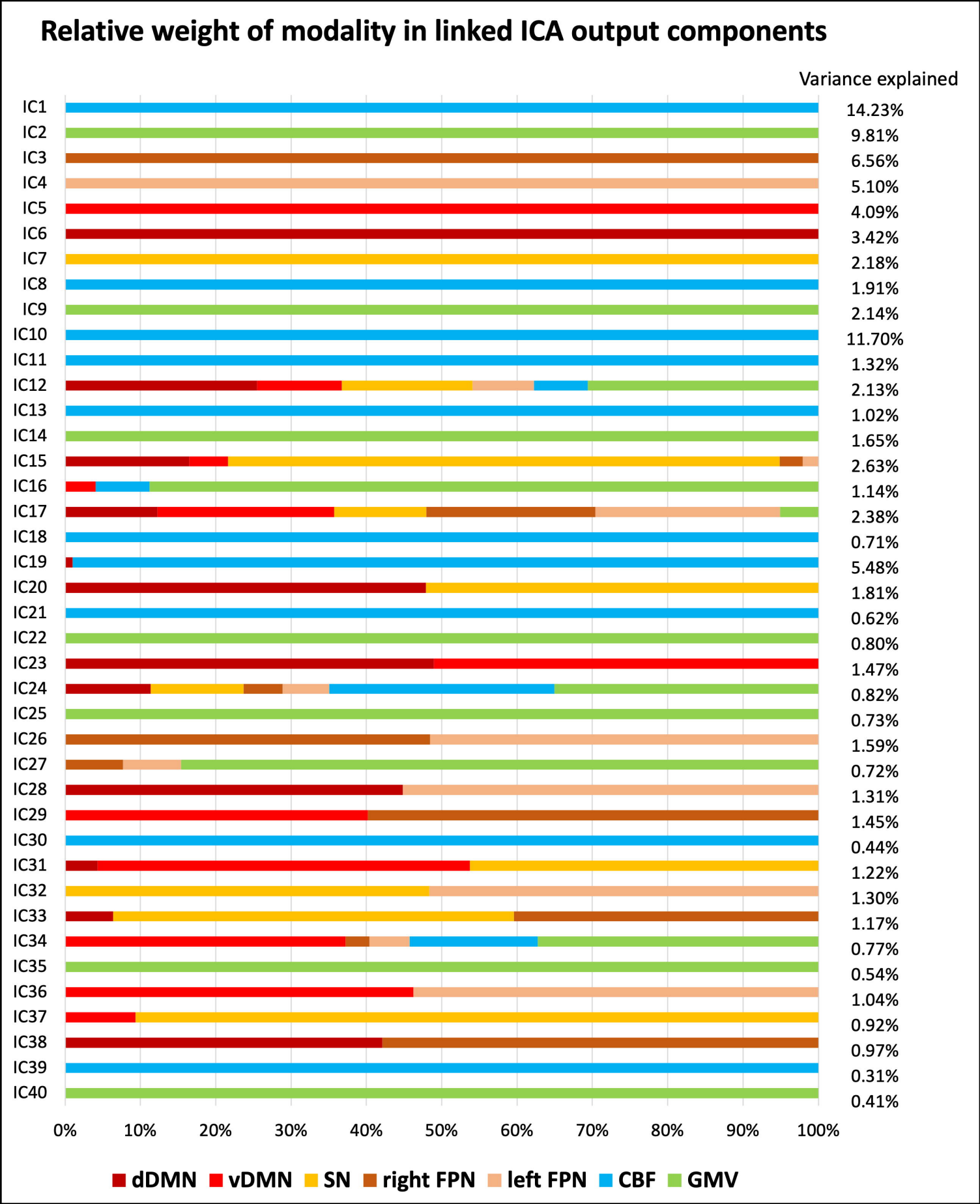
Relative weight of modality in linked ICA output components
Variance explained
IC1 14.23%
IC2 9.81%
IC3 6.56%
IC4 5.10%
IC5 4.09%
IC6 3.42%
IC7 2.18%
IC8 1.91%
IC9 2.14%
IC10 11.70%
IC11 1.32%
IC12 2.13%
IC13 1.02%
IC14 1.65%
IC15 2.63%
IC16 1.14%
IC17 2.38%
IC18 0.71%
IC19 5.48%
IC20 1.81%
IC21 0.62%
IC22 0.80%
IC23 1.47%
IC24 0.82%
IC25 0.73%
IC26 1.59%
IC27 0.72%
IC28 1.31%
IC29 1.45%
IC30 0.44%
IC31 1.22%
IC32 1.30%
IC33 1.17%
IC34 0.77%
IC35 0.54%
IC36 1.04%
IC37 0.92%
IC38 0.97%
IC39 0.31%
IC40 0.41%
0% 10% 20% 30% 40% 50% 60% 70% 80% 90% 100%
dDMN vDMN SN right FPN left FPN CBF GMV

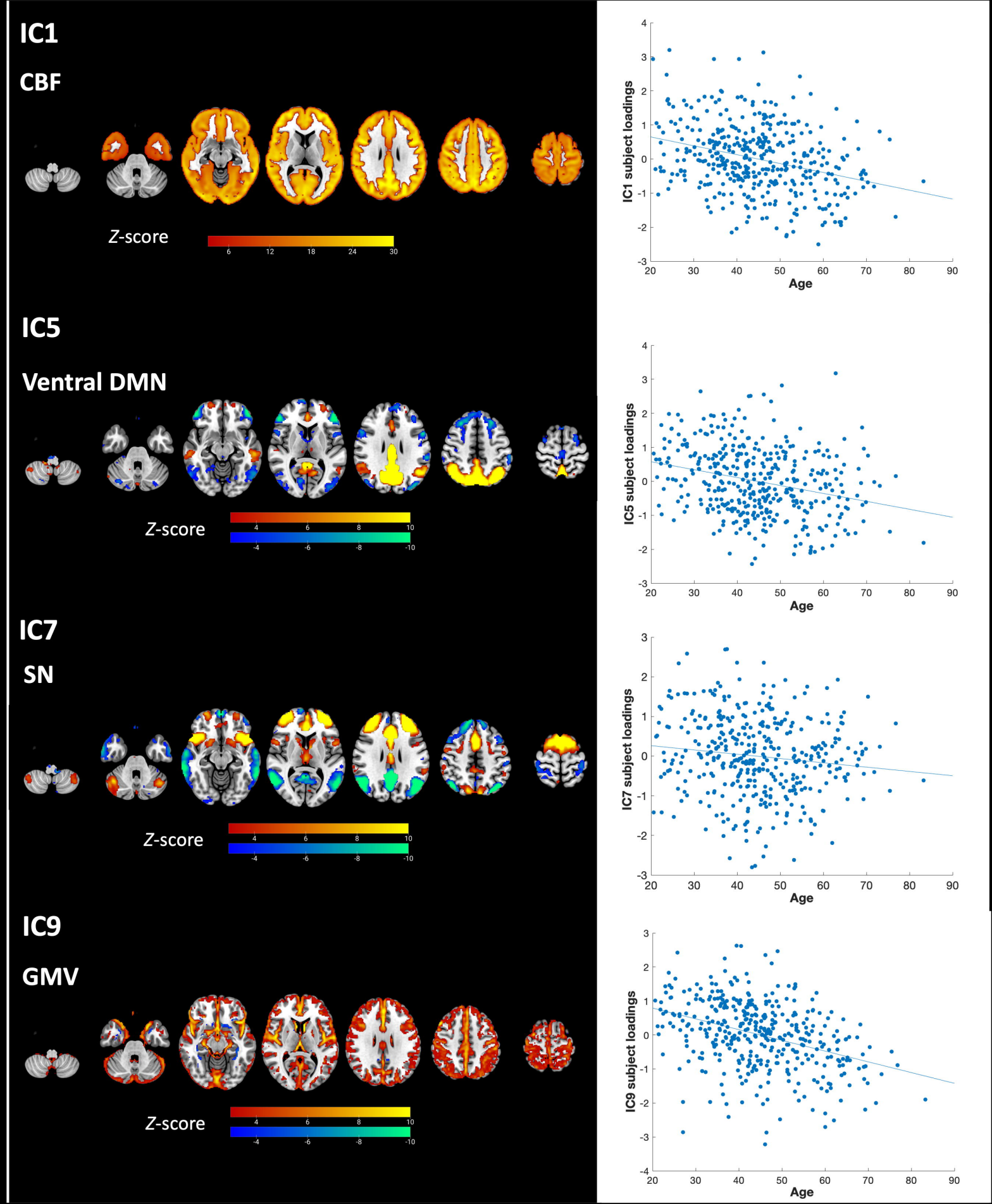
IC1
CBF
Z-score
6
12
18
24
30
IC1 subject loadings
Age
IC5
Ventral DMN
Z-score
4
6
8
10
-4
-6
-8
-10
IC5 subject loadings
Age
IC7
SN
Z-score
4
6
8
10
-4
-6
-8
-10
IC7 subject loadings
Age
IC9
GMV
Z-score
4
6
8
10
-4
-6
-8
-10
IC9 subject loadings
Age

IC4

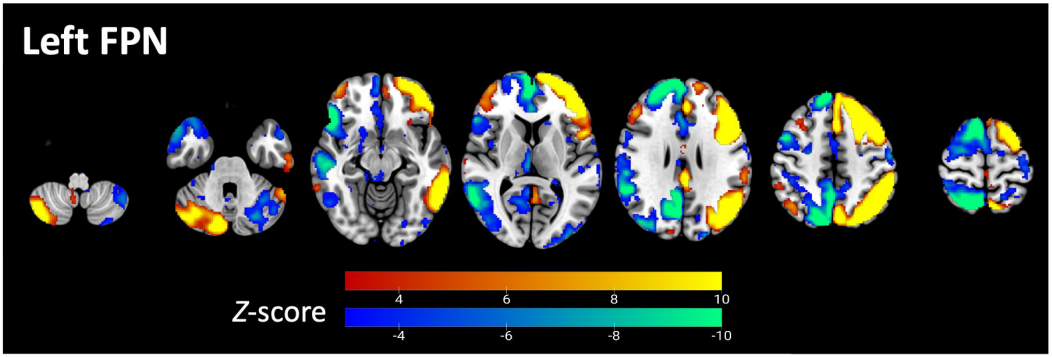
Left FPN
Z-score
4
6
8
10
-4
-6
-8
-10

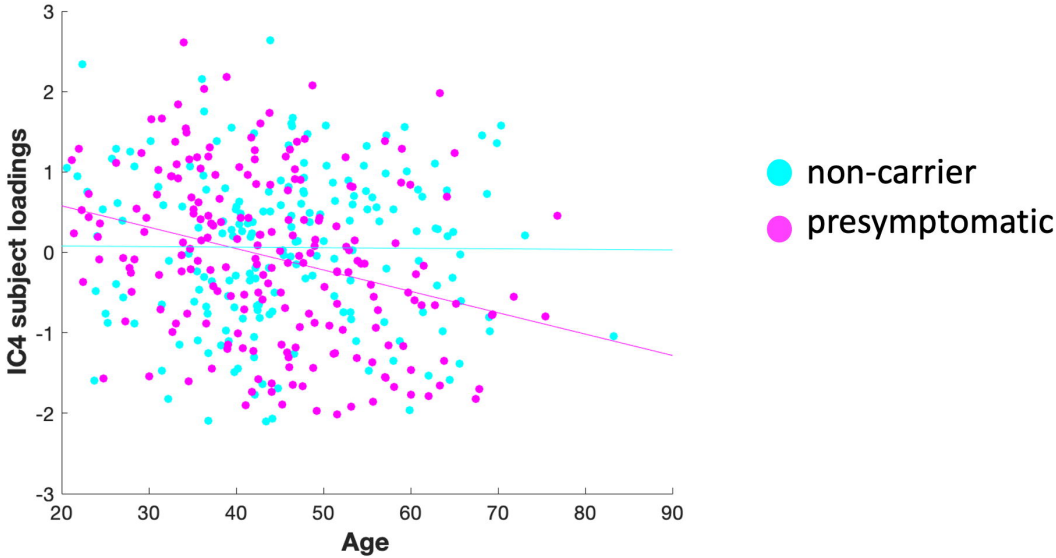
IC4 subject loadings
Age
3
2
1
0
-1
-2
-3
20
30
40
50
60
70
80
90
non-carrier
presymptomatic

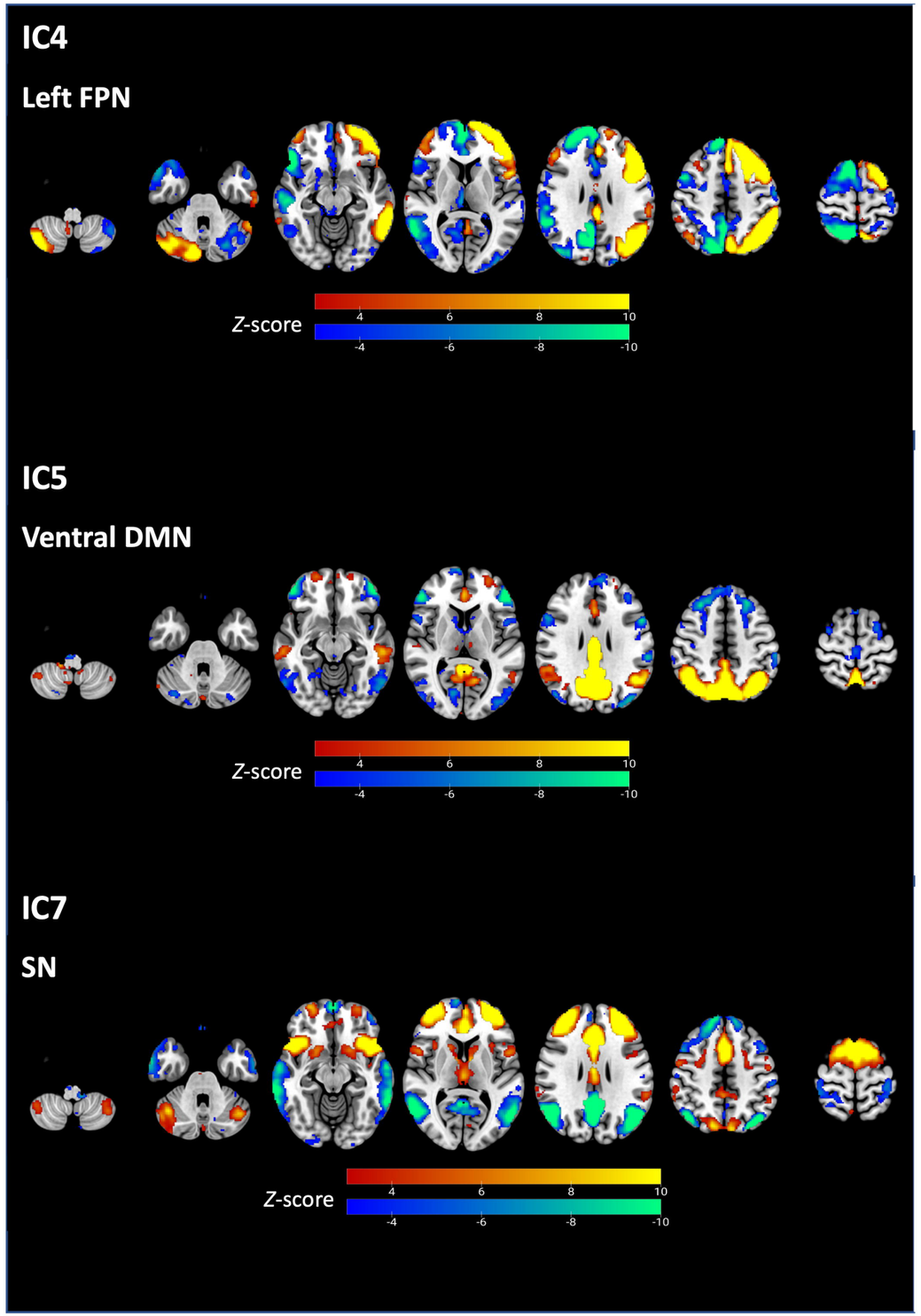
IC4
Left FPN
Z-score
4 6 8 10
-4 -6 -8 -10
IC5
Ventral DMN
Z-score
4 6 8 10
-4 -6 -8 -10
IC7
SN
Z-score
4 6 8 10
-4 -6 -8 -10

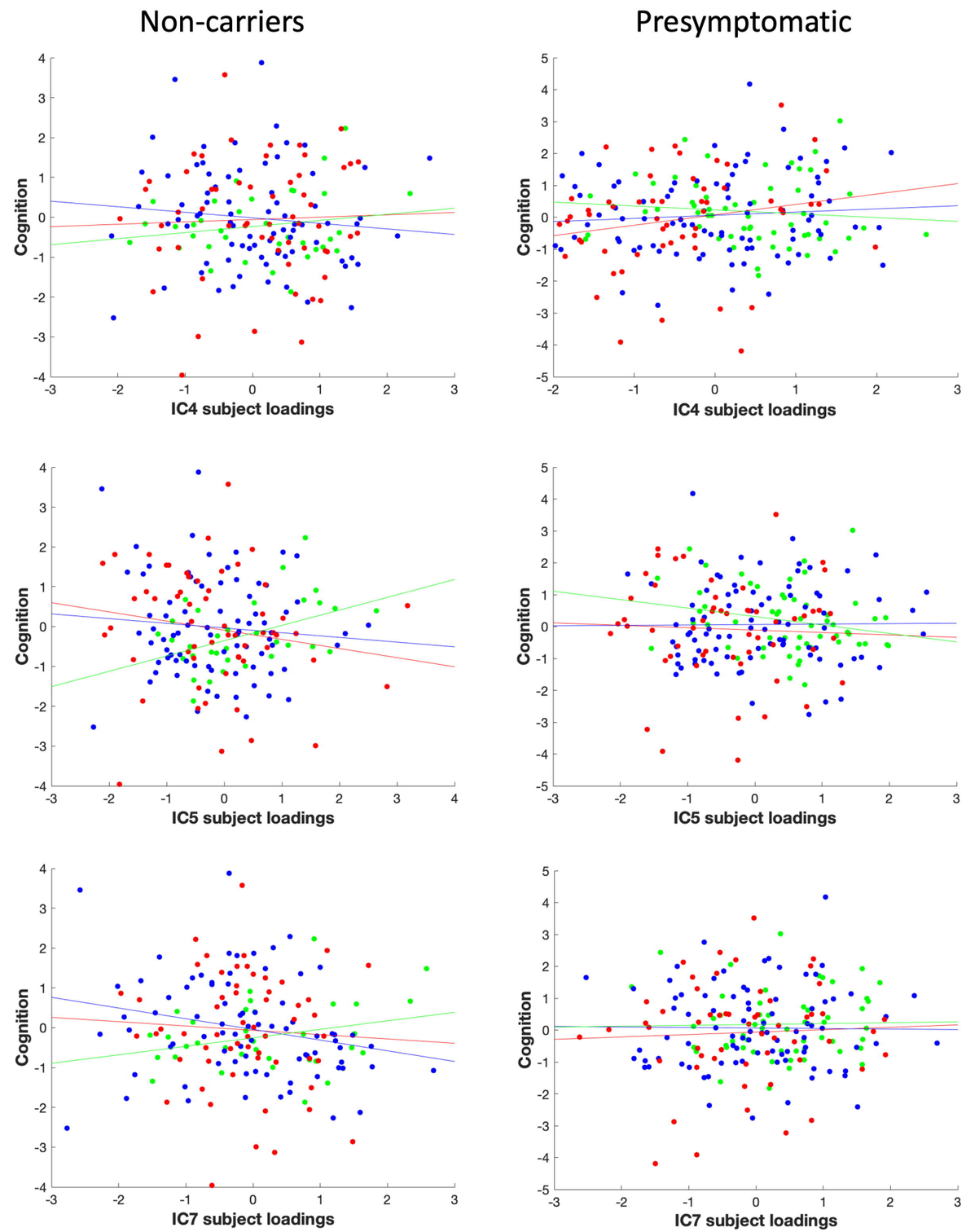
Non-carriers
Presymptomatic
Cognition
IC4 subject loadings
IC5 subject loadings
IC7 subject loadings
21-35 years old
36-49 years old
50-76 years old